MATERIALS PHYSICS AND MECHANICS RESEARCH ARTICLE

Submitted: May 22, 2026 **Revised: June 29, 2026** **Accepted: July 9, 2026**

Statistical approaches for studying the strength properties of ZSM-5-based extrudates with different zeolite framework Si/Al ratios

D.I. Lashchenko, O.O. Zaikina, R.G. Kukushkin✉, V.A. Yakovlev

Boreskov Institute of Catalysis SB RAS, Novosibirsk, Russia

✉ roman@catalysis.ru

ABSTRACT

The influence of ZSM-5 composition on the mechanical strength of extruded alumina–ZSM-5 catalysts is studied. For samples with zeolite content ranging from 0 to 95 % and Si/Al ratios of 11.5, 15, and 25, the compressive strength was measured and described by a normal distribution and Weibull statistics. Strength depends non-linearly on zeolite content, peaking at 20 wt. % for all series. ZSM-5 with Si/Al = 15 yields statistically higher strength than Si/Al = 11.5 or 25. The Weibull modulus increases with zeolite content, indicating a more homogeneous granule structure. The observed differences are attributed to the particle size distributions: maximal strength occurs when the bimodal ZSM-5 distribution efficiently complements the pseudoboehmite particles, ensuring optimal packing and binding.

KEYWORDS

extrusion • mechanical strength • Weibull distribution • ZSM-5 • alumina • statistical analysis.

***Funding**. This work was supported by the Russian Science Foundation (project № 25-23-01310).*

***Acknowledgements.** The authors thank E.A. Mel'gunova for textural properties determination, E.A. Suprun for SEM characterization, and O.A. Bulavchenko for XRD analysis.*

Citation: Lashchenko DI, Zaikina OO, Kukushkin RG, Yakovlev VA. Statistical approaches for studying the strength properties of ZSM-5-based extrudates with different zeolite framework Si/Al ratios. *Materials Physics and Mechanics*. 2026;54(4): 77–97.
http://dx.doi.org/10.18149/MPM.5442026_8

Introduction

Zeolite-based catalysts are widely used in many industrial processes, particularly in petrochemistry and oil refining [1–4]. However, synthetic zeolites are typically obtained as powders with a characteristic micrometer-sized particle distribution. The use of zeolite powders in industrial reactors leads to increased hydrodynamic resistance of the catalyst bed and, consequently, to the emergence of local pressure drops within the reactor [5]. To address this issue, zeolites are shaped into solid bodies of various forms, ranging from several millimeters to several centimeters, using binders [6,7]. The granule size directly affects the diffusion of reactants and products, as well as the mechanical properties due to the increased probability of defect formation [8]; each industrial process has its own optimal catalyst granule size and shape [9].

Due to its simplicity and high throughput, extrusion is the most common method for zeolite shaping [10,11]. The extrusion process results in the immobilization of zeolite particles within the volume of the shaped body; the binder serves to provide the desired shape and mechanical strength, although the choice of the binder system critically impacts both the macroscopic integrity and the microscopic catalytic properties [12,13]. Pseudoboehmite has found widespread use as a binder [14–16]. To prepare an extruded

© D.I. Lashchenko, O.O. Zaikina, R.G. Kukushkin, V.A. Yakovlev, 2026.
Publisher: Peter the Great St. Petersburg Polytechnic University
This is an open access article under the CC BY-NC 4.0 license (https://creativecommons.org/li-censes/by-nc/4.0/)

zeolite-containing support, a paste is prepared by mixing powders of the binder and zeolite with the addition of a peptizer; this paste is then extruded through a die to form individual granules, which undergo subsequent thermal treatment [17]; the size and shape of the extrudates are determined by the die.

Mechanical strength is one of the key operational characteristics of an industrial catalyst [11,18–20]. However, the strength of a porous solid is generally determined by a combination of numerous factors (density and strength of individual contacts between crystallites and their agglomerates, porosity, defects, etc. [21]). During operation, catalyst pellets in the bed experience both thermal and mechanical stresses [22–24]. In such composite systems, thermal stresses and the difference in the coefficients of thermal expansion of the components can significantly affect the temperature dependence of mechanical strength. Furthermore, the operating temperature conditions directly determine the critical parameters of fracture toughness and the fracture behavior of the material [25,26]. The fracture of catalyst granules in the reactor leads to local pressure drops, flow disruption, and contamination of the product with fine granule fragments [27,28].

Catalysts based on porous oxides are brittle materials that do not exhibit plastic deformation prior to mechanical failure [29]. Several studies have established correlations between strength and porosity, as well as with the size of cracks in the material structure [30,31]. As recent modeling studies show, the local stress concentration near microstructural defects, such as pores or interphase boundaries of inhomogeneities, acts as a key factor initiating microcrack growth in composite ceramic matrices [32,33]. However, the diversity of defects (pores, dislocations, cracks) in terms of their size, shape, and spatial orientation within the granule volume leads to significant scatter in the strength values of individual pellets within a catalyst batch [34,35]. Therefore, most methods for determining the strength of adsorbent or catalyst particles are statistical in nature.

According to standards [36,37], quantitative strength characteristics of shaped catalysts and adsorbents are typically described by parameters such as the mean mechanical strength of a sample and its standard deviation under the assumption of a normal data distribution. This approach can adequately describe the mechanical properties of extrudates with simple shape [29]. However, in the case of excessively high scatter in the strength values of individual granules and a strength distribution that significantly deviates from normal, this statistical approach may fail to represent the actual mechanical properties of different catalyst and support samples [20,38]. Conversely, the use of probabilistic distributions enables the prediction of the probability of catalyst granule failure under a specific load. An indispensable tool in this context is the Weibull distribution, widely used for the statistical description of the strength of brittle materials (e.g., glass, ceramics) [39–42], including catalyst pellets [32]. This approach is based on the "weakest link theory": the most "critical" defect in the material under an applied load will control the strength, akin to a chain that fails if its weakest link breaks [43]. It is important to note that the "critical" defect in the structure is not necessarily the largest; its position, shape, and orientation within the granule play crucial roles [29].

Currently, there is a growing interest in investigating the mechanical properties of zeolite-containing extrudates using the Weibull distribution. Salem and colleagues, in a series of studies [44,45], demonstrated the applicability of the Weibull distribution for describing the mechanical strength of Raschig ring-shaped extrudates composed of

natural zeolite, bentonite, and kaolin. Their work studied the influence of both the zeolite-bentonite-kaolin ratio and the calcination temperature on the mechanical properties. Wu et al. [17] used the two-parameter Weibull distribution to investigate various extrusion parameters of hierarchically porous ZSM-5, such as the content of the binder and peptizer, as well as the extrusion speed, on mechanical strength. It was shown that the optimal properties of the shaped ZSM-5 are achieved using 33 wt. % pseudoboehmite, 13 wt. % nitric acid, and an extrusion speed of 50 rpm. The study [46] demonstrated that a reduction in the content of the binder and peptizer leads to a decrease in the mechanical strength of the resulting alumina and bio-templated ZSM-5-based extrudates. Furthermore, key fabrication steps such as drying and calcination conditions were recently optimized for ZSM-5 extruded catalysts using response surface methodology to maximize mechanical reliability and Weibull modulus [47,48]. In previous work [49], it was demonstrated that the mechanical strength of γ-Al_2O_3-ZSM-5 extrudates of varying composition non-linearly depends on the ZSM-5 content (Si/Al = 11.5). Maximum strength was achieved at 20 wt. % zeolite and was higher than that of pure extruded alumina. It was shown that residual nitrate groups in pseudoboehmite allow shaping without the use of an additional peptizer. Similar non-linear dependence of mechanical strength on the zeolite content was also recently reported for composite supports based on γ-Al_2O_3 and mordenite [50].

Although the Si/Al ratio in the zeolite framework is a key characteristic determining the acidity of the aluminosilicate system [51,52], its effect on the mechanical properties of zeolite-containing extrudates has not been previously studied. Therefore, this work is primarily focused on understanding the influence of the Si/Al ratio in the ZSM-5 framework on the mechanical properties of Al_2O_3-ZSM-5 extrudates with varying zeolite content, with application of normal and Weibull distributions for statistical strength data analysis.

Materials and Methods

Materials

Powders of pseudoboehmite and ZSM-5 zeolite were used to prepare the support granules. The pseudoboehmite was obtained via nitrate-ammonia precipitation; the preparation method and its characterization are described in the previous study [49]. Commercial ZSM-5 samples with different Si/Al ratios were used in the NH_4^+-form (Zeolyst International, CBV 2314, Si/Al = 11.5; CBV 3024E, Si/Al = 30; CBV 5524G, Si/Al = 50). Parent ZSM-5 samples in their H-form after calcination are marked as Z(y), where y is the corresponding Si/Al ratio.

Extrusion procedure

In this work, three series of granular composites A-xZ(y) were prepared, where A is γ-Al_2O_3, Z is ZSM-5, x = 0, 10, 20, 30, 50, 60, 70, 95, and means mass fraction of zeolite in the initial powder mixture, and y = 11.5, 15, 25, and means Si/Al ratio in the zeolite framework. Thus, within one series, the pseudoboehmite-to-ZSM-5 ratio was varied, while the series differed from each other in the Si/Al ratio of the zeolite. The sample containing

no ZSM-5 (x = 0) was designated as A. All samples were prepared by extrusion; a typical procedure is described below.

For each sample, powders of pseudoboehmite and ZSM-5 were kneaded with the addition of water to form a homogeneous paste using an overhead laboratory stirrer. The paste was then transferred to a manual laboratory extruder equipped with a 4 mm diameter die. To ensure a consistent manual extrusion rate, 7–8 mm of paste was extruded through the die before cutting. The resulting extrudates were subsequently dried at 120 °C (1 h), followed by calcination at 550 °C (4 h, 10 °C/min) in an air atmosphere. After thermal treatment, cylindrical extrudates with a length of 5–6 mm were obtained. For the preparation of the sample A, the initial mixture contained no zeolite; paste kneading and thermal treatment were carried out under the same conditions.

Characterization of samples

Phase composition, textural properties, and scanning electron microscopy. Powder X-ray diffraction (XRD) patterns of the extrudates were collected on an X'tra diffractometer (Thermo Fisher Scientific, Switzerland) in the 2θ range of 4–75° with a step size of 0.02° and a scanning rate of 1 °/min using a Mythen2 X 1D linear detector (Dectris, Switzerland). CuKα radiation (λ = 1.5418 Å) was used. The average size of coherent scattering regions (CSR) for the zeolite was estimated from the Scherrer equation using the reflection at 2θ ≈ 23.1°, which corresponds to the Miller indices (101) for the MFI topology.

The textural properties of the extrudates were determined by low-temperature nitrogen adsorption-desorption measurements using an ASAP-2400 instrument. Prior to the measurements, the samples were pretreated in a N_2 flow at 300 °C for 20 h to remove adsorbed moisture from the surface. The specific surface area (*SSA*) was calculated using the Brunauer-Emmett-Teller (BET) model based on multilayer adsorption. The mesopore characteristics (V_{meso}) were determined from the desorption branch using the Barrett-Joyner-Halenda (BJH) method. The micropore characteristics (S_{micro}, V_{micro}) were evaluated using the t-plot method. The total pore volume (V_{total}) was calculated as the volume of nitrogen adsorbed at a relative pressure of P/P_0 = 0.995. The surface of the polished cross-sections of the support granules was examined using a Solaris S900 FIB-SEM dual-beam scanning electron microscope (Tescan, Czech Republic) at a probe electron energy of 20 keV.

The shrinkage of the extrudates (post-shrinkage, PS_{4h}) after 4 h of thermal treatment and subsequent cooling to room temperature was calculated using Eq. (1), in accordance with GOST 34206-2017 [53]:

$$PS_{4h} = \frac{d_0 - d_1}{d_0} \times 100\%, \quad (1)$$

where d_0 is the diameter of the extruder die (mm), and d_1 is the diameter of the extrudates after thermal treatment and cooling (mm).

Radial crush strength (normal and Weibull distributions). The radial crush strength of the extrudates was determined using a DVT BP D NN testing machine (DEVOTRANS, Turkey) in accordance with the ASTM D6175-03 standard [36]. Each extrudate, after measuring its length and diameter, was compressed between two rigid parallel plates at a speed of 10 mm/min. The measurement was performed by recording the applied force (*F*) immediately preceding the failure of the extrudate, which was accompanied by a sharp drop in load. The sample size for each specimen A-xZ(y) was 50 granules.

Based on normal distribution, the mechanical crush strength per millimeter of extrudate length (x) was determined using Eq. (2):

$$x = \frac{F}{L}, \quad (2)$$

where F is the force required to break the extrudate (N), and L is the length of the extrudate (mm).

Subsequently, the mean mechanical strength (X) and standard deviation (SD) were calculated using Eqs. (3) and (4), respectively:

$$X = \frac{\sum x}{n}, \quad (3)$$

$$SD = \sqrt{\frac{\sum (X - \bar{X})^2}{n-1}}, \quad (4)$$

where $\sum (X - \bar{X})^2$ is the sum of squared deviations of each force per millimeter from the mean force per millimeter for the sample, and n is the sample size.

The measurement error (ΔX) was calculated using Eq. (5):

$$\Delta X = t_{0.95} \cdot \sqrt{\frac{D}{n}}, \quad (5)$$

where $t_{0.95}$ is the Student's coefficient for a confidence level of 0.95, D is the sample variance, and n is the sample size.

The coefficient of variation (CV) was calculated using Eq. (6):

$$CV = \frac{SD}{X} \cdot 100\%. \quad (6)$$

The crush strength per square millimeter of the extrudate cross-sectional area (x_s) was determined using Eq. (7):

$$x_s = \frac{4F}{\pi d_1^2}, \quad (7)$$

where F is the force required to break the extrudate (N), and d_1 is the diameter of the extrudate (mm).

For the statistical analysis of the strength characteristics, the two-parameter Weibull distribution (8) was employed, which accurately describes the mechanical properties of solid porous catalysts [20,29,54]:

$$P = 1 - exp\left[-\left(\frac{F}{\sigma_0}\right)^m\right], \quad (8)$$

where P is the probability of extrudate failure, F is the applied force (N) required for extrudate failure, m is the Weibull modulus (shape parameter), and σ_0 is the scale parameter (N).

The shape and scale parameters were estimated using linear regression (LR). The probability of extrudate failure, P, was estimated using the probability estimator (9) (also known as the plotting position [55]), which yields low error for sample sizes greater than 20 [38,56–58]:

$$P_i = \frac{i - 0.5}{n}, \quad (9)$$

where P_i is the probability of failure of the i-th extrudate, i is the i-th (ranked) order of failure, n is the total number of specimens tested.

Particle size distribution of powders. The particle size distribution in the powders was measured by laser diffraction using a SALD 2101 instrument (Shimadzu Corp., Japan) equipped with a wet dispersion unit, in accordance with ASTM D4464-15 standard [59]. A suspension was prepared from a representative sample of the test powder in a solvent-

dispersant medium (H_2O-C_2H_5OH). The resulting suspension was subjected to ultrasonic treatment for 1 min and intensive stirring for 2 min to break down particle agglomerates. Subsequently, an aliquot of the prepared sample suspension was placed into the instrument's measurement cell. The volume-based median diameter, *MV* (mean particle size, μm), and standard deviation, *SD* (μm), were calculated using Eqs. (10) and (11), respectively:

$$\lg MV = \frac{1}{100}\sum_{i=1}^{n} q_i \frac{\lg x_i + \lg x_{i+1}}{2}, \quad (10)$$

$$SD = \sqrt{\left(\frac{1}{100}\sum_{i=1}^{n} q_i \frac{\lg x_i + \lg x_{i+1}}{2}\right) - (\lg MV)^2}, \quad (11)$$

where x_i is the particle diameter (μm), and q_i is the percentage in the differential distribution (%).

Results and Discussion

The obtained A-xZ(y) extrudates were studied by XRD (Fig. 1). All investigated samples showed reflections at 2θ = 7.9°, 8.8°, 23.0°, 23.4°, and 24°, corresponding to the diffraction pattern of a zeolite with MFI topology [60,61] [PDF 44-0003] and an orthorhombic space group symmetry [62]. Thus, the crystalline structure of the zeolite with different framework Si/Al ratios is preserved during the shaping process at zeolite contents of both 20 and 50 wt. %. At low ZSM-5 content (up to 20 wt. %, Fig. 1(a)), the diffraction patterns show broad reflections at 2θ = 46.0° and 66.7° [PDF 02-1420], corresponding to the alumina binder phase. These reflections practically disappear (Fig. 1(b)) with increasing ZSM-5 content, and the diffraction patterns of the extrudates become almost identical to those of the parent ZSM-5 samples [63]. A more complete description of the physicochemical properties of the A-xZ(11.5) series samples is presented in our previous work [49].

The average CSR sizes for ZSM-5 within the A-xZ(y) extrudates are calculated and are presented in Table 1. It can be seen that for the zeolite within the extrudates of a given series, the average CSR size falls within the margin of error when compared to the corresponding parent ZSM-5 sample and does not depend on the zeolite content.

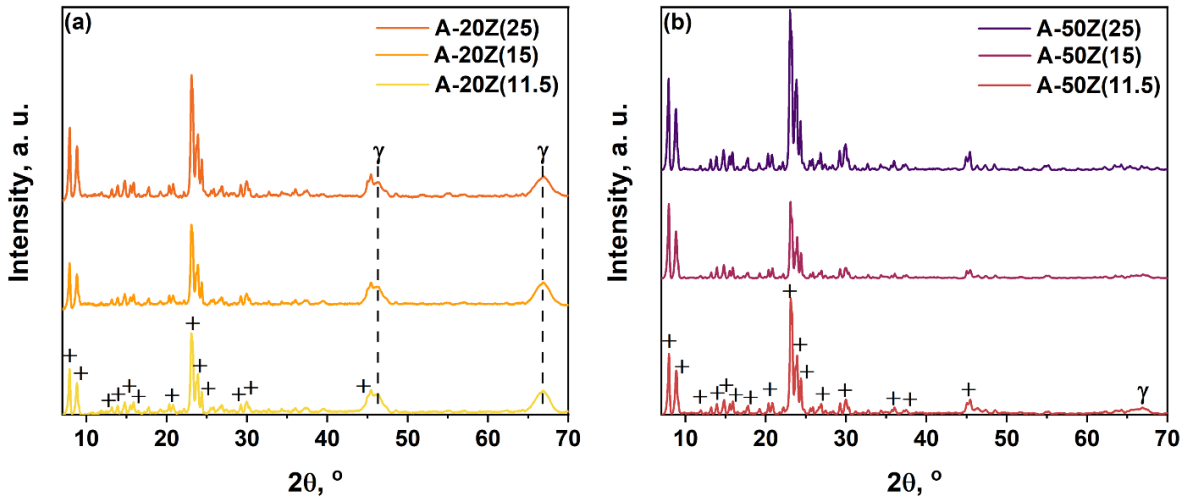


Fig. 1. XRD patterns of the extrudates: (a) diffraction patterns of the A-20Z(y) samples, (b) diffraction patterns of the A-50Z(y) samples. Reflections from ZSM-5 are marked with a + symbol, and those from γ-Al_2O_3 are marked with a γ symbol

Table 1. Average *CSR* sizes of ZSM-5 for the A-xZ(y) samples and the parent Z(y) samples in the H-form

Sample or series	Min. CSR size, Å	Max. CSR size, Å
A-xZ(11.5)	470	490
Z(11.5)	490	
A-xZ(15)	520	550
Z(15)	470	
A-xZ(25)	350	390
Z(25)	340	

The average CSR size for the parent Z(11.5) and Z(15) zeolites is approximately the same, while for the Z(25) sample it is somewhat lower, indicating a smaller crystallite size.

The textural properties of the A-xZ(y) extrudates and the parent ZSM-5 powders are presented in Table 2. Parent ZSM-5 samples with different Si/Al ratios possess comparable SSA and contributions from the micropore surface area to the total surface area. Furthermore, an increase in the Si/Al ratio leads to an increase in V_{total}, which is also accompanied by an increase in the contribution of mesopore volume to V_{total}. These data may indicate an increase in the average mesopore diameter with increasing Si/Al ratio in the zeolite framework. The $S_{external}/SSA$ values for the Z(11.5), Z(15), and Z(25) samples are 0.09, 0.10, and 0.12, respectively, indicating an increase in intercrystalline mesoporosity in this series. The influence of the Si/Al ratio on the textural properties of zeolites is noted in the literature [64], with the *SSA* reported either to increase with the Si/Al ratio [48] or to pass through a maximum [65].

Table 2. Textural properties of the A-20Z(y) and A-60Z(y) extrudates, and the parent Z(y) samples

Sample	*SSA*, m^2/g	S_{micro}/SSA	V_{total}, cm^3/g	V_{meso}/V_{total}	V_{micro}/V_{total}
A-20Z(11.5)	271	0.19	0.611	1.02	0.04
A-20Z(15)	257	0.18	0.583	1.03	0.04
A-20Z(25)	270	0.17	0.552	1.00	0.04
A-60Z(11.5)	355	0.54	0.354	0.74	0.23
A-60Z(15)	372	0.45	0.411	0.74	0.18
A-60Z(25)	378	0.50	0.405	0.75	0.20
Z(11.5)	438	0.91	0.217	0.24	0.76
Z(15)	425	0.90	0.247	0.36	0.63
Z(25)	432	0.88	0.281	0.46	0.56

Nevertheless, the textural properties (in particular, the pore volume) for the A-xZ(y) extrudates are largely determined by the alumina binder, especially at low ZSM-5 content. Some differences in the mesoporosity of the parent ZSM-5 are leveled out due to the fact that the intrinsic mesoporosity of ZSM-5 is negligible compared to that of γ-Al_2O_3. Thus, as can be seen from Table 2, in the case of the A-xZ(y) extrudates, the zeolite content determines *SSA* and S_{micro}, while the binder content governs V_{total} and, in particular, V_{meso} values.

Extrudates with the same ZSM-5 content but different framework Si/Al ratios (exemplified by the A-20Z(y) and A-60Z(y) samples) possess comparable values of specific surface area, micropore surface area, and micropore volume. The differences are less pronounced for the A-20Z(y) samples due to their lower zeolite content. It can be seen that the A-60Z(15) sample exhibits the lowest S_{micro}/SSA and V_{micro}/V_{total} ratios, which may be explained by greater blocking of the zeolite micropores by binder particles, for instance, due to the formation of a denser packing within the granule [66].

The SEM images (Fig. 2) demonstrate a uniform distribution of ZSM-5 within the extrudates at different zeolite content. In the higher magnification images (Fig. 2(a,b)), differences in the microstructure of the samples with different ZSM-5 contents are clearly visible. At a content of 20 wt. % (Fig. 2(a)), the zeolite is distributed within the binder matrix as individual particles, whereas in the sample with 50 wt. % zeolite (Fig. 2(b)), the microstructure becomes more porous, and the ZSM-5 agglomerates are coated with layers of binder. In the latter sample, well-defined micrometer-sized cavities are clearly visible, resulting from the presence of free space between the zeolite agglomerates. In the lower magnification images (Fig. 2(c,d)), a homogeneous structure of the obtained granules can be observed; no cracks, large voids, or ZSM-5 agglomerates are detected. For the sample A-50Z(15) (Fig. 2(d)), micrometer-sized cavities (black in the image) are also observed. The formation of such cavities with increasing ZSM-5 content is expected to lead to a deterioration of the mechanical properties of the extrudates.

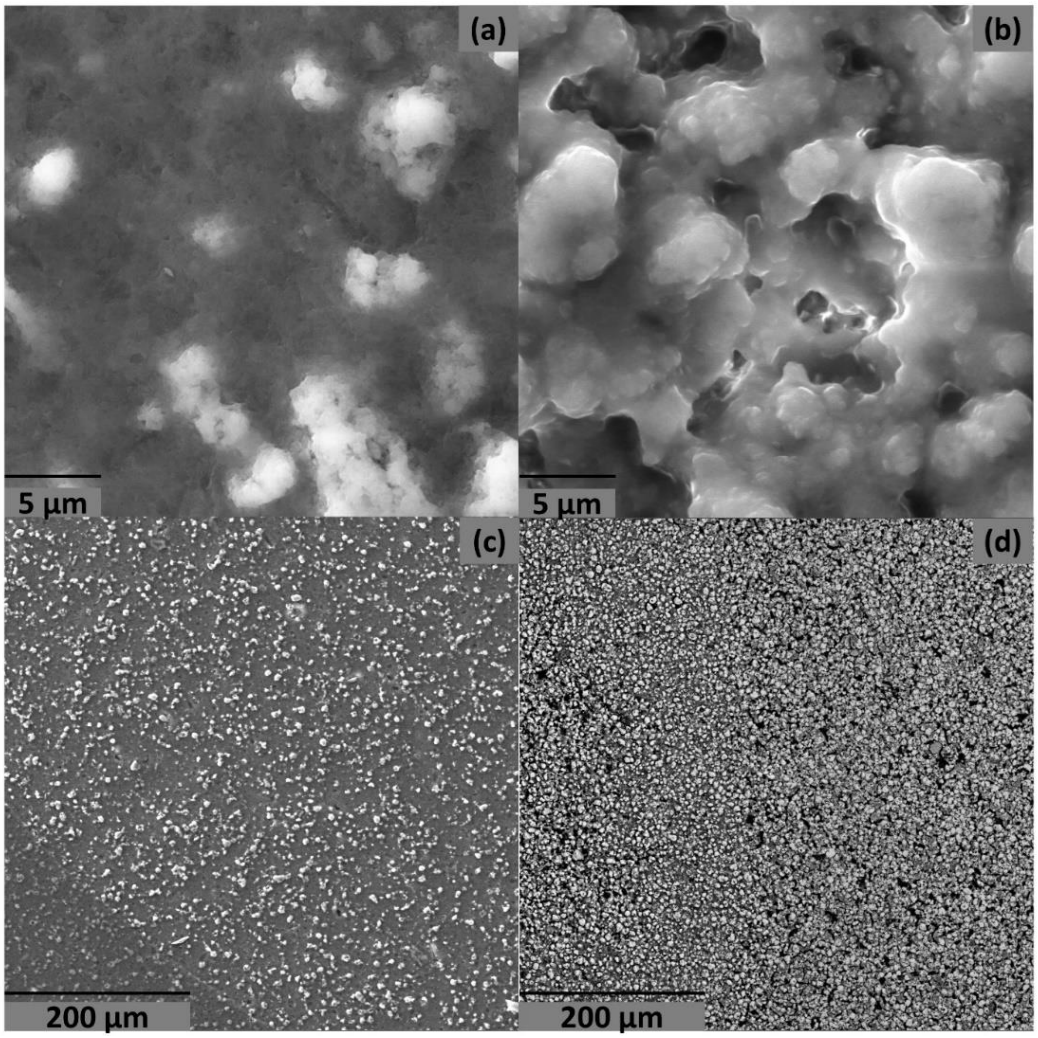


Fig. 2. SEM micrographs: (a, c) the sample A-20Z(15), (b, d) the sample A-50Z(15)

The radial crush strength was measured for all obtained composite supports A-xZ(y), as well as for the sample A, in accordance with ASTM D6175-03. The macroscopic morphology of the extrudates before and after the strength test is shown in Fig. 3. It is clearly seen that extrudates with different zeolite content fracture differently.

For instance, the sample A (pure alumina) forms only small, irregularly shaped fragments upon failure. The addition of 20 wt. % zeolite (the sample A-20Z(15)) results in more regular fragments formed during extrudate failure, both perpendicular and parallel to the generatrix. In turn, (the sample A-50Z(15) fails primarily along the generatrix, forming almost identical, symmetrical fragments. Presumably, the sample without zeolite additive has a higher concentration of internal stresses compared to the ZSM-5-containing extrudates, which crack predominantly along the generatrix. This differing fracture pattern of the resulting fragments may indicate a more homogeneous and isotropic structure of the A-xZ(15) extrudates compared to the shaped alumina [67].

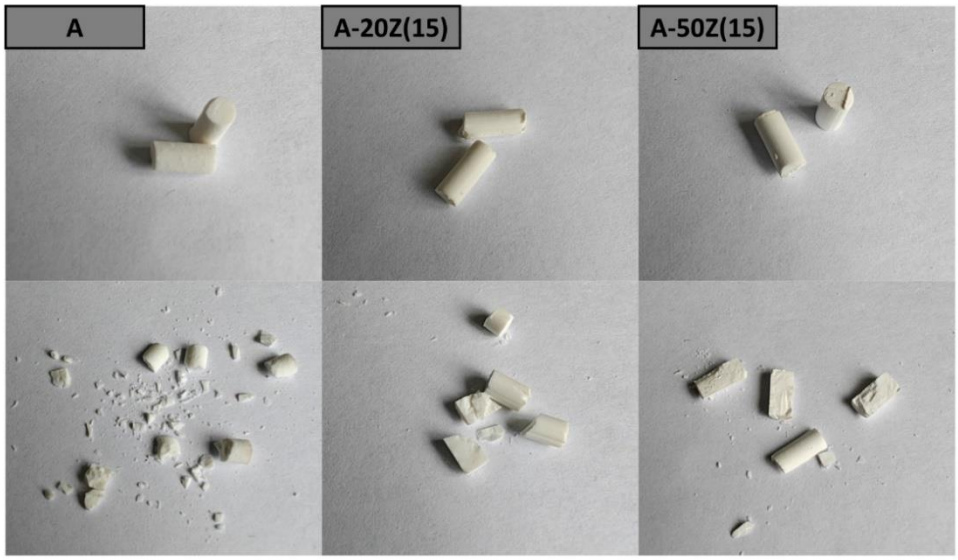


Fig. 3. Visual appearance of the A-xZ(15) extrudates before (top) and after (bottom) the radial crush strength test

The mean mechanical strength, calculated based on the normal distribution according to ASTM D6175-03 (Eqs. (2)–(5)) for the A-xZ(y) extrudates, exhibits a non-linear dependence on the ZSM-5 content across the entire range of Si/Al ratios (Fig. 4(a)).

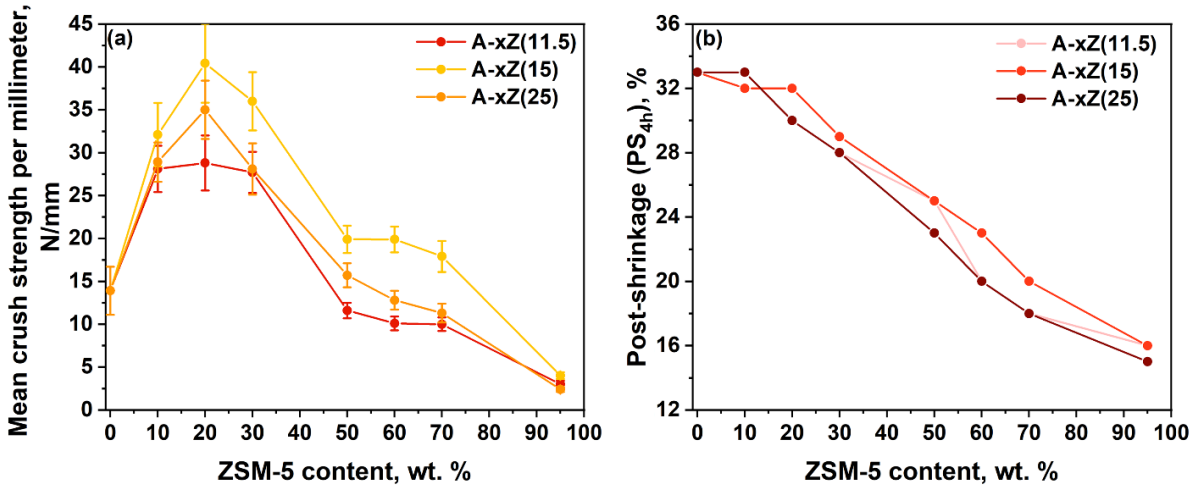


Fig. 4. Dependence of the mechanical properties of the extrudates on their composition: (a) mean radial crush strength; (b) post-shrinkage

As the zeolite content in the extrudates increases to 30 wt. %, a significant increase (up to 3-fold) in the mean mechanical strength is observed compared to the sample A,regardless of the framework Si/Al ratio. For the A-xZ(15) series, the mean mechanical strength of the A-50Z(15) - A-70Z(15) samples is also higher than that of the sample A. In all cases, the maximum values of the mean mechanical strength are achieved at 20 wt. % ZSM-5 in the extrudates; a further increase in zeolite content leads to a decrease in strength.

The A-xZ(25) series demonstrates a strength reduction closest to linear over the 20–95 wt. % zeolite interval, while the A-xZ(11.5) and A-xZ(15) series exhibit a pronounced plateau in the 50–70 wt. % ZSM-5 range. In turn, the A-95Z(y) samples possess similar mechanical strength values. Thus, all series show a qualitatively similar non-linear dependence of strength on zeolite content; quantitatively, however, the strength values differ significantly for samples with the same ZSM-5 content but different Si/Al ratios.

The dependence of PS_{4h}, calculated using Eq. (1), on the ZSM-5 content in the extrudates of different series is presented in Fig. 4(b). The post-shrinkage after thermal treatment is due to the removal of water from pseudoboehmite; consequently, it is determined by its content in the extrudates. It can be observed that for all samples, the dependence of PS_{4h} on composition is nearly linear; the shrinkage of the granules in the A-xZ(15) series is somewhat greater than that of the other samples.

The strength characteristics of the A-xZ(y) extrudates were analyzed using the two-parameter Weibull distribution (8). Taking the double logarithm of Eq. (8), it can be rewritten in the form of Eq. (12) [56]:

$$\ln\ln\left(\frac{1}{1-P}\right) = m\ln F - m\ln\sigma_0. \quad (12)$$

It can be seen that the relationship between $\ln F$ and $\ln\ln\left(\frac{1}{1-P}\right)$ is linear, which allows for the calculation of the Weibull modulus (m, also referred to as the shape parameter) and the scale parameter (σ_0), which are empirical material constants [68], using the LR method [17,69,70]. The calculated parameters are subsequently used to construct the continuous Weibull distribution for estimating the critical crush strength values $F_{i\%}$, which correspond to the percentage of the weakest granules in the sample. It is known that the size of extrudates with regular geometry (spheres, cylinders) contributes to the scatter in strength data [20]; given the nearly identical shrinkage (and, consequently, diameter) and length of 5–6 mm for extrudates with the same zeolite content, this factor can be neglected. In turn, it has been reported that a sample size of 50 granules is sufficient to achieve acceptable accuracy in estimating the Weibull parameters [56,71]. The results of the analysis using Weibull statistics are presented in Fig. 5.

Figure 5(a,c) presents the Weibull distributions for the samples A, A-20Z(y), and A-50Z(y), respectively. It can be observed that the obtained data generally reflect the trend in the changes in the strength characteristics of the extrudates presented in Fig. 4(a). The Weibull distribution represents a transformation of the dataset on the strength of individual granules into a probability function, which can further be used to predict extrudate failure under a specific applied load [8,29,43]. Consequently, the higher the applied load at a low probability of failure, the stronger the sample is overall. Indeed, the A-20Z(y) samples undergo mechanical failure at significantly higher loads than the sample A.

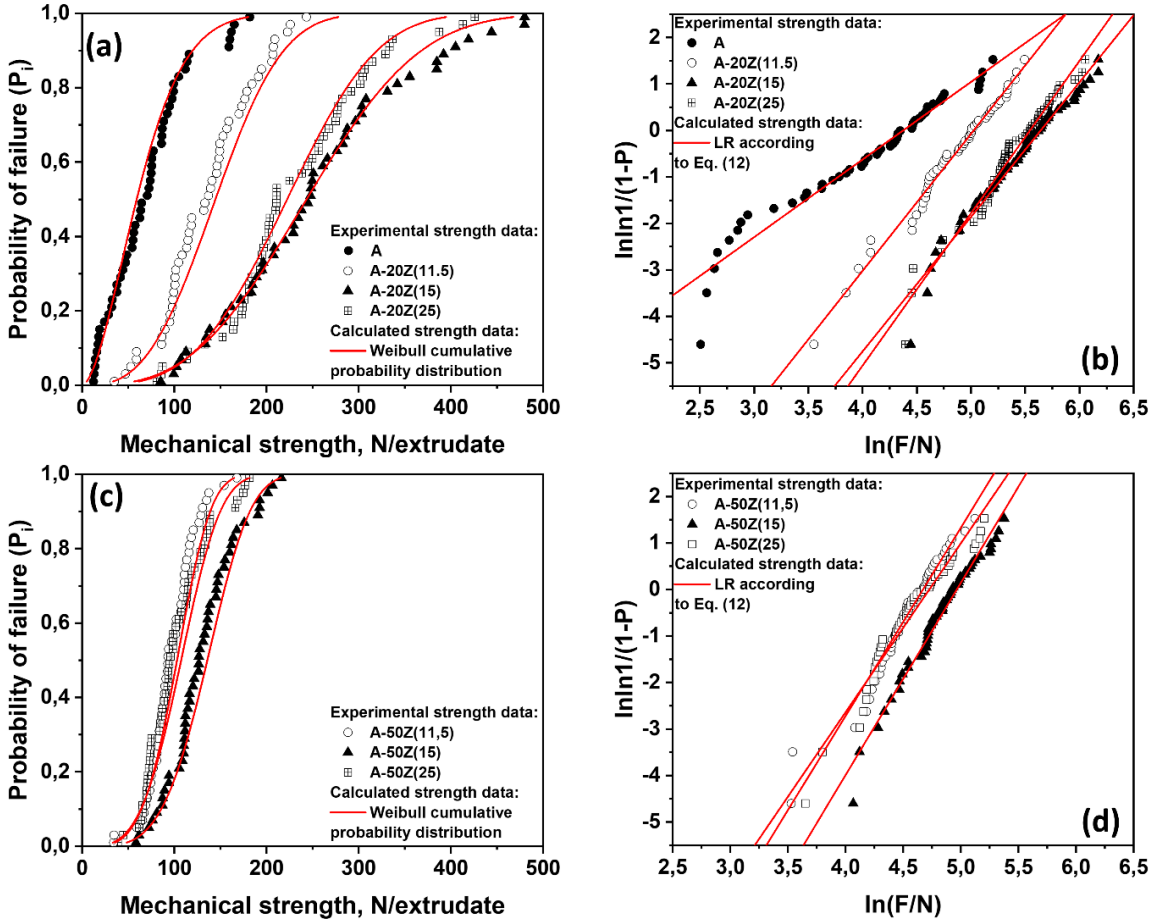


Fig. 5. Strength characteristics of the extrudates: (a,b) Weibull distribution and Weibull plot for the samples A, A-20Z(11.5), A-20Z(15), and A-20Z(25), respectively; (c,d) Weibull distribution and Weibull plot for samples A-50Z(11.5), A-50Z(15), and A-50Z(25), respectively. Experimental data are denoted by points, calculated data are denoted by lines

Within the sample set (Fig. 5(a)), the mechanical properties of the extrudates deteriorate in the order A-20Z(15) > A-20Z(25) > A-20Z(11.5) > A, which is also consistent with the changes in the mean radial crush strength values for these samples. A similar conclusion can be drawn for the A-50Z(y) samples (Fig. 5(c)). It can be observed that the sample A-50Z(15) is the least susceptible to mechanical failure among the A-50Z(y) samples; the mechanical properties also deteriorate in the order A-50Z(15) > A-50Z(25) > A-50Z(11.5). The statistical data obtained from the analysis for the studied samples are presented in Table 3.

Table 3. Statistical strength characteristics of the A-xZ(y) extrudates.

Sample	*m*	σ_0, N	R^2	$F_{1\%}$, N	$F_{5\%}$, N	$F_{10\%}$, N
A	1.7	73.3	0.951	4.9	12.8	19.1
A-20Z(11.5)	2.9	164.0	0.984	33.7	58.7	75.4
A-20Z(15)	2.9	276.1	0.971	57.0	98.9	126.3
A-20Z(25)	3.3	248.4	0.972	62.8	101.6	125.4
A-50Z(11.5)	4.0	112.7	0.960	35.9	53.7	64.1
A-50Z(15)	4.1	148.4	0.975	48.5	71.3	86.2
A-50Z(25)	3.6	118.8	0.952	33.3	51.8	64.1

It is noteworthy that on the Weibull plots (Fig. 5(b,d)) for the alumina sample, the experimental data points in the left region lie on a straight line with a high slope. This may indicate a bimodal distribution due to the presence of an additional type of defect in the granule structure [40], resulting in these granules possessing extremely low strength. However, these points are not outliers (see below) or a second component of the sample population (Supporting Information, Table S1).

It can be observed that for all samples, the coefficients of determination (R^2) exceed 0.95, indicating that the studied systems are adequately described by Weibull statistics. It is known that the dimensionless Weibull modulus m (shape parameter) determines the scatter in the strength distribution of the extrudates. This parameter is related to the number and/or size of physical defects on the surface and in the volume of the brittle sample [68,72,73]. The higher the value of the Weibull modulus, the narrower the distribution of granule strength, and the smaller the deviation of the strength of individual granules from the mean sample strength value towards significantly lower values, and vice versa. In our case, the Weibull parameter values ranged from 1.7 to 4.1, while the typical range for technical ceramic materials is from 5 to 20 [71]. The scale parameter σ_0 corresponds to the load applied to the sample at a cumulative failure probability of 63.2 % and, thus, characterizes its strength: the higher the σ_0, the stronger the sample [8,69].

It can be seen that the Weibull modulus generally increases with increasing ZSM-5 content in the extrudates, indicating a more homogeneous granule structure at higher zeolite loadings. For the A-20Z(y) and A-50Z(y) samples with the same zeolite content but different Si/Al ratios, the m value differs only slightly. The increase in ZSM-5 content reduces the heterogeneity in the extrudate structure, likely due to a reduction in internal stresses during the crystallization of γ-Al_2O_3 from AlOOH upon thermal treatment. During the formation of the γ-Al_2O_3 crystalline structure, primary needle-like particles coalesce and interweave via chemical interaction, forming crystallization contacts [74]; these contacts are considered weaker than the bonds within the crystallites themselves [31]. Simultaneously, internal stresses arise due to the mutual growth of crystallites towards each other, which can lead to microcracks and voids [21,75]. Residual stresses may form during the cooling of the extrudates, associated with the anisotropic thermal expansion

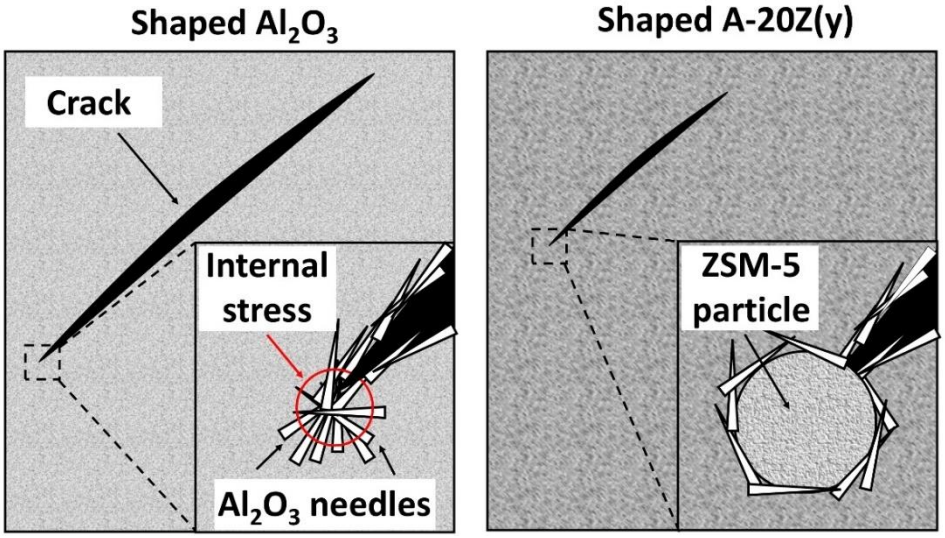


Fig. 6. Schematic structure of γ-Al_2O_3-based and γ-Al_2O_3-ZSM-5-based extrudates

of the material in the axial and radial directions [57]. As a result, various stresses concentrate at the boundaries of other defects, such as cracks, and under applied load can form a critical defect responsible for granule failure [76]. The addition of zeolite presumably stabilizes the resulting binder structure, leading to a more homogeneous morphology and improved mechanical properties [8]. This effect may be achieved both through the "dilution" of internal stresses within the granule volume and by reducing the size of cracks (whose formation, however, may itself be a consequence of stress development [38]), since a larger crack size leads to lower strength [68]. This assumption is schematically illustrated in Fig. 6.

It is important to note that the calculated values of the Weibull modulus for the A-xZ(y) extrudates are invariant to their size. The use of the strength per unit length, x, and the strength per unit cross-sectional area, x_s, of the extrudate (calculated using Eqs. (2) and (7), respectively, as schematically shown in Fig. 7) in Eq. (12) instead of F values yields virtually identical values of the Weibull modulus (Supporting Information, Table S2). Physically, this may indicate both a uniform distribution of defects within the extrudates and their isotropy throughout the volume. Given the homogeneous distribution of ZSM-5 in the extrudates, this finding correlates well with the aforementioned assumptions regarding mechanical internal stresses in the alumina binder, which is uniformly distributed throughout the granule volume.

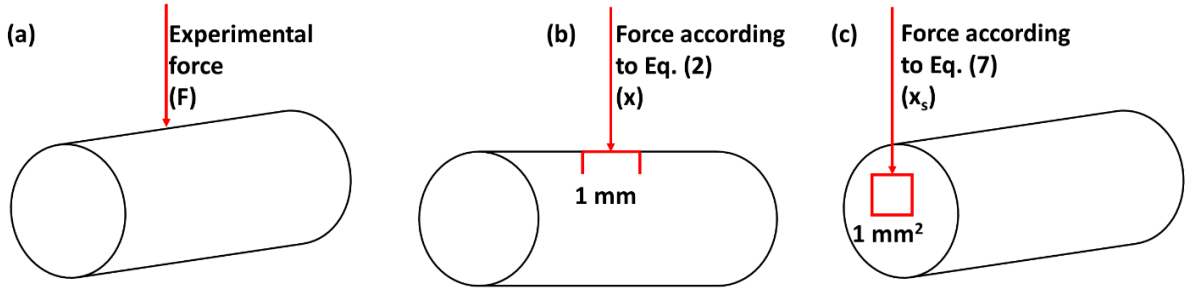


Fig. 7. Schematic definition of mechanical strength: (a) experimental values for the whole extrudate, (b) strength per unit length, (c) strength per unit cross-sectional area

The scale parameter σ_0 also generally reflects the overall trend in the strength characteristics of the samples obtained from the mean radial crush strength values (Fig. 4). The data show that the force required to fracture the granules of the A-20Z(y) and A-50Z(y) samples at a probability of 63.2 % increases significantly compared to that of alumina. Thus, the overall strength decreases in the order A-50Z(15) > A-50Z(25) > A-50Z(11.5) > A. It is noteworthy that in Fig. 4, samples A-50Z(11.5) and A-50Z(25) demonstrate a mean strength comparable to that of alumina within the margin of error, whereas according to Weibull statistics, they are significantly stronger. It can be assumed that over the range from A to A-50Z(y), a change in the type of granule strength distribution occurs: the increase in the Weibull modulus m is associated with a narrowing of the distribution and an increase in homogeneity, which may indicate an approach towards a normal distribution. In the case of alumina, the distribution is likely highly skewed, which may impede the correct comparison of strength characteristics using the mean mechanical strength. More detailed reasoning will be provided below.

It is well-established that the strength of a catalyst bed is determined by its weakest granules, making their mechanical characteristics a more important parameter than, for example, the mean strength of the entire sample batch [22,32]. Based on the Weibull distribution for the samples, the critical crush strength values corresponding to extrudate failure probabilities of 1, 5, and 10 % (parameters $F_{1\%}$, $F_{5\%}$, and $F_{10\%}$, respectively) were estimated. The higher the values of these parameters, the stronger the most mechanically unreliable granules are. The lowest values are observed for the sample A. For the A-20Z(y) samples, the values generally follow the overall strength trend; however, the $F_{1\%}$, $F_{5\%}$, and $F_{10\%}$ values are close for samples A-20Z(15) and A-20Z(25), indicating nearly identical strength characteristics of the weakest granules in these samples. A different trend is observed for the 50 wt. % ZSM-5 samples: all critical values for the sample A-50Z(15) are significantly higher than those for A-50Z(11.5) and A-50Z(25), for which they are practically identical; these data are consistent with the change in the scale parameter σ_0 for these samples, indicating their comparable strength. Thus, in terms of critical strength values, samples A-20Z(15) and A-20Z(25), as well as A-50Z(11.5) and A-50Z(25), possess nearly identical strength, despite noticeable differences in their mean strength. In contrast, the sample A is significantly less strong compared to A-50Z(11.5) and A-50Z(25), despite their comparable mean strength.

A box-and-whisker diagram (box plot) of the strength characteristics of the extrudates is presented in Fig. 8. The statistical data are provided in Table 4; for comparison, the mean strength values obtained according to the ASTM D6175-03 standard using Eq. (3) are also indicated. It can be observed that in the case of alumina (Fig. 8(a)), the distribution is indeed asymmetric; the median and mean are nearly identical and are significantly shifted towards the less strong granules, which is also indicated by the high *SD*. For the A-20Z(11.5) samples, the mean and median values are also close, while the distributions themselves become more symmetrical. The range between the minimum (Q1 - 1.5IQR) and maximum (Q3 + 1.5IQR) values widens; however, this does not contradict the previously calculated Weibull modulus values. Upon transitioning from A to A-20Z(y), the actual distribution narrows in accordance with the Weibull statistics, which is confirmed by the decrease in the coefficients of variation (*CV*). Nevertheless, the box plot demonstrates the emergence

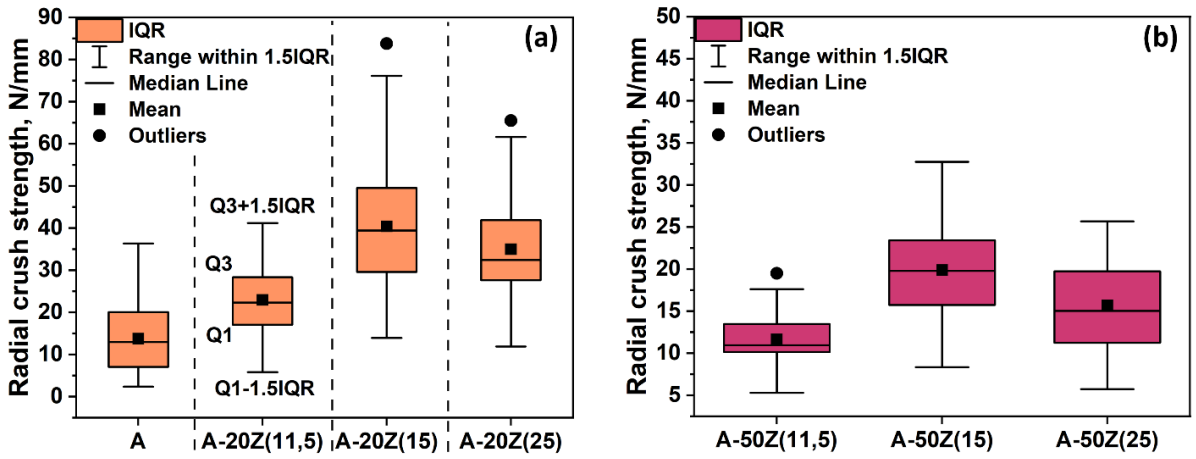


Fig. 8. Box plots of the mechanical strength of the samples: (a) A, A-20Z(11.5), A-20Z(15), and A-20Z(25); (b) A-50Z(11.5), A-50Z(15), and A-50Z(25)

Table 4. Statistical data on the strength distribution of the extrudates

Sample	Mean strength, N/mm	*SD*, N/mm	*CV*, %	Median, N/mm	*IQR*, N/mm
A	13.7	8.9	65.0	2.4	13.1
A-20Z(11,5)	23.0	8.4	36.5	22.3	11.3
A-20Z(15)	40.4	16.2	40.1	39.4	19.9
A-20Z(25)	35.0	12.0	34.3	32.4	14.3
A-50Z(11,5)	11.6	3.0	25.9	10.9	3.4
A-50Z(15)	19.9	5.6	28.1	19.8	7.7
A-50Z(25)	15.7	5.0	31.8	15.0	8.5

of individual granules that are both much stronger and much weaker than the mean value. Furthermore, it can be seen that for the A-20Z(15) and A-20Z(25) samples, the minimum strength values are close, indicating similar strength characteristics of the weakest granules and consistent with the conclusions drawn from the analysis of the critical values $F_{5\%}$ and $F_{10\%}$ for these samples.

With an increase in the ZSM-5 content to 50 wt. %, a significant narrowing of the strength distribution of the sample granules is observed (Fig. 8(b)). This is consistent with the increase in the Weibull modulus for these samples and likely indicates that higher zeolite content significantly reduces the probability of forming both very strong and very weak granules. Furthermore, it is evident that the distributions become nearly symmetrical, leading to discrepancies in the assessment of the mechanical properties of the samples A, A-50Z(11.5), and A-50Z(25) when using the mean mechanical strength versus Weibull statistics. Given the symmetrical distributions for the zeolite-containing samples, the mean mechanical strength should adequately reflect their mechanical characteristics. However, it can be assumed that the true mean strength of alumina would be lower than the value calculated using Eq. (3).

It is widely accepted that the binder content has a decisive influence on the mechanical strength of zeolite catalysts [13,77,78], which is consistent with the results of this work. However, the data obtained in this study using several statistical data processing methods also point to a significant role of the zeolite, which initially possesses virtually no mechanical strength, in the mechanical properties of the extrudates. Thus, while the potential for forming the strongest (and weakest) granules is indeed determined by the binder content (samples with lower ZSM-5 content are stronger than those with higher content), the addition of zeolite is capable of increasing the strength of individual granules on average, likely due to a reduction in the concentration of internal stresses within the granule, leading to the formation of a more homogeneous structure.

Nevertheless, the obtained data explain the change in mechanical strength depending on the ZSM-5 content in the extrudates but, however, do not explain the different strength characteristics of samples with the same zeolite content but different framework Si/Al ratios. The preservation of the ZSM-5 crystalline structure in the A-xZ(y) samples, their comparable textural properties, as well as similar Weibull moduli for the A-20Z(y) and A-50Z(y) samples have been demonstrated. This raises the question: how then do extrudates with different Si/Al ratios in the ZSM-5 framework differ? To answer this, powders of pure pseudoboehmite and the parent ZSM-5 samples were analyzed by laser diffraction (Fig. 9) to determine the average particle size of the powders. It is known

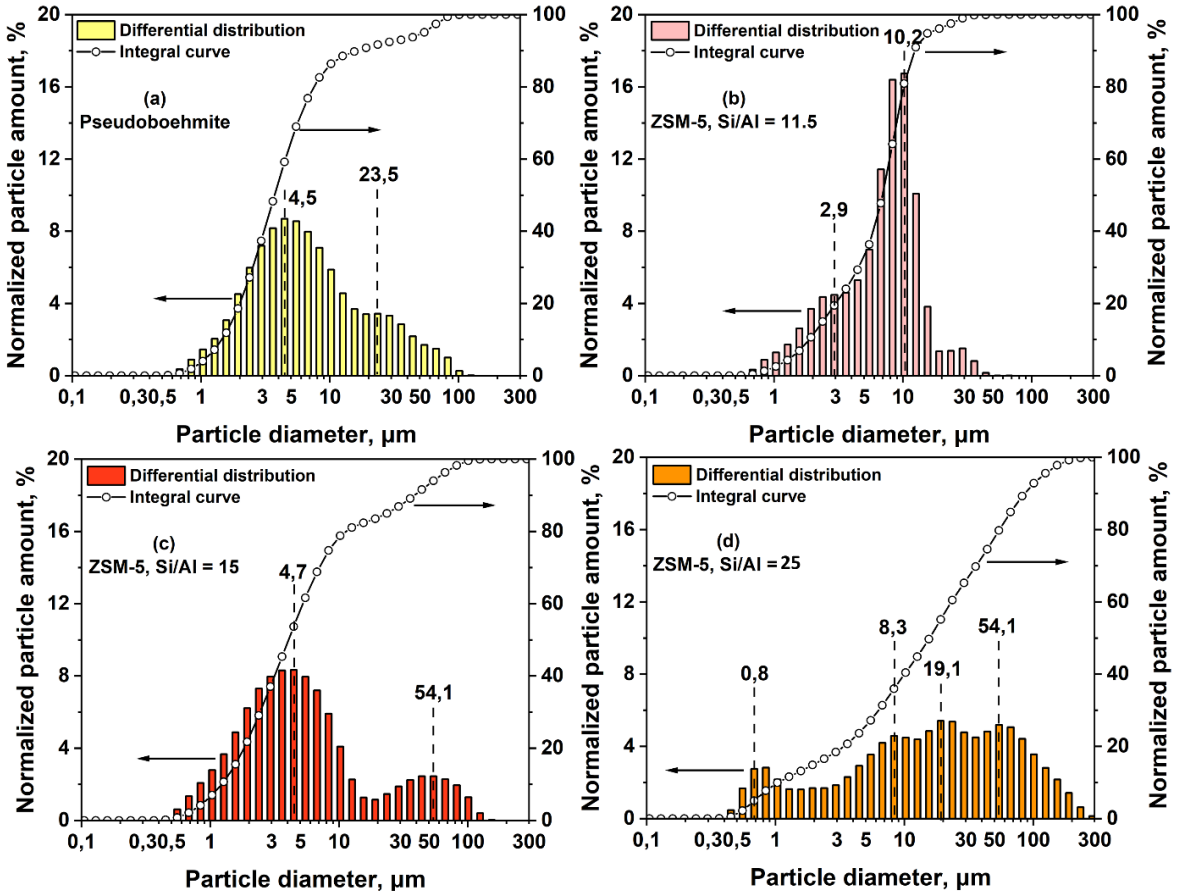


Fig. 9. Particle size distributions of the powders: (a) -pseudoboehmite, (b) -Z(11.5), (c) -Z(15), (d) -Z(25). The distribution modes are indicated by numbers

that the particle size of a powder significantly influences the mechanical properties of porous materials [79,80]. For instance, a combination of smaller and larger alumina particles can lead to higher packing density and, consequently, improved mechanical properties of the extrudates [81]. It is believed that for most effective binding in extrudates, zeolite particles should be sufficiently fine, and their size distribution in the powder should be sufficiently broad. At the same time, zeolite particles should be larger than the binder particles to achieve denser packing and, thus, improved mechanical properties. However, overly large particles (> 150 μm) of brittle material (alumina, zeolite) promote the formation of microcracks [82], while fine binder particles contribute to the formation of a strong structure in the shaped body [83].

It can be observed that the distributions obtained using Eqs. (10) and (11) are multimodal, with maxima of the average particle size distribution both below 10 μm and above 50 μm; the statistical data are presented in Table S3 (Supporting Information). From Fig. 9(a), it can be seen that pseudoboehmite consists predominantly of small particles (≈ 85 % below 10 μm) with a maximum at 4.5 μm; however, larger particles with a size exceeding 20 μm are also observed. Thus, it can be expected that to achieve the best mechanical properties of the A-xZ(y) extrudates, the zeolite particles in the powder should also exhibit a bimodal distribution with correspondingly larger maxima.

The ZSM-5 sample with Si/Al = 11.5 exhibits (Fig. 9(b)) a relatively narrow particle size distribution, with ≈ 70 % of particles in the range of 3 to 10 μm. The content of particles up to 3 μm in size is comparable to that of the pseudoboehmite sample; however, particles larger than 20 μm are practically absent. This combination may lead to the formation of unfilled intercrystalline cavities of the zeolite in the extrudates at higher zeolite content and, consequently, reduce the strength. This assumption is supported by the largest pore volume of the samples in this series, obtained from the textural characterization.

For the ZSM-5 sample with Si/Al = 15, a pronounced bimodal particle size distribution is observed (Fig. 9(c)), with maxima at 4.7 and 54.1 μm. The content of particles up to 10 μm in size is similar to that of the pseudoboehmite powder; particles larger than 10 μm are significantly larger compared to those in pseudoboehmite. The finer binder particles can fill the spaces between the zeolite particles, thereby ensuring effective binding of ZSM-5 (increasing the mechanical strength), which is confirmed by the somewhat higher PS_{4h} values for all granules in this series. The greater post-shrinkage leads to tighter contact between the binder and the zeolite, resulting in blockage of the ZSM-5 micropores, which is consistent with the textural properties from Table 2.

Finally, the ZSM-5 sample with Si/Al = 25 exhibits (Fig. 9(d)) a broad particle size distribution ranging from 0.3 to 300 μm, with ≈ 10 % of particles falling within the 100 to 300 μm range. This may lead to the formation of microcracks in the granules and thus reduce their strength. This assumption is consistent with the experimentally determined strength characteristics of the A-xZ(25) extrudates, which are lower than those of the A-xZ(15) samples.

Conclusion

In this work, extrudates based on ZSM-5 of various compositions A-xZ(y), where A = γ-Al_2O_3, Z = ZSM-5, x = 0–95 is the mass fraction of zeolite in the initial mixture, and y = 11.5, 15, 25 is the Si/Al ratio in the zeolite framework, were systematically studied. XRD analysis demonstrated the preservation of the zeolite's crystalline structure within the extrudates. It was shown that extrudates with the same ZSM-5 content but different Si/Al ratios possess comparable textural properties. Samples with a higher zeolite content exhibit a higher specific surface area, while a higher alumina binder content leads to an increased specific pore volume.

The mechanical properties of the extrudates were investigated using various statistical data analysis approaches, such as normal distribution (mean strength, ASTM D6175-03), Weibull distribution, and descriptive statistics. All employed methods demonstrate a qualitatively non-linear dependence of the mechanical strength of the extrudates on the ZSM-5 content, with maximum strength achieved at 20 wt. % zeolite regardless of the framework Si/Al ratio (samples A-20Z(y)). Quantitatively, the strength characteristics varied significantly between samples with the same zeolite content but different Si/Al ratios in the framework. The statistical approaches used in this work provide different data on the strength characteristics of the extrudates, which, in combination, complement each other. Thus, to obtain the most complete and illustrative

information on the mechanical properties of the A-xZ(y) extrudates, it is advisable to combine all three statistical approaches.

It has been demonstrated that the introduction of zeolite into the alumina binder matrix can play a significant role in altering the strength characteristics of the extrudates. On the one hand, the strength of the granules is determined by the binder content due to the formation of the strongest granules, as demonstrated by the normal distribution strength statistics. On the other hand, the addition of zeolite is capable of increasing the strength of individual granules on average, leading to a narrower and more symmetrical distribution, likely due to a reduction in internal stress concentration within the granule, as evidenced by the Weibull distribution statistical data. This indicates the possibility of a synergistic effect between γ-Al_2O_3 and ZSM-5 at their specific ratio, which is particularly pronounced for the A-20Z(y) samples and results in the improvement of their mechanical properties.

For the A-xZ(11.5) and A-xZ(25) series, it has been demonstrated that zeolite particles that are either too small or too large compared to the binder particles lead to a reduction in strength. The matching of the particle size distributions of the pseudoboehmite and zeolite powders in the case of the A-xZ(15) series results in more efficient binding and denser particle packing, which is accompanied by greater shrinkage and leads to increased mechanical strength.

CRediT authorship contribution statement

Daniil I. Lashchenko: writing – original draft, writing – review & editing, investigation; **Olesya O. Zaikina**: writing – review & editing, investigation; **Roman G. Kukushkin**: writing – review & editing, conceptualization, supervision; **Vadim A. Yakovlev**: supervision, data curation.

Conflict of interest

The authors declare that they have no conflict of interest.

References

1. Pérez-Ramírez J, Christensen CH, Egeblad K, Groen JC. Hierarchical zeolites: enhanced utilisation of microporous crystals in catalysis by advances in materials design. *Chemical Society Reviews.* 2008;37(11): 2530–2542.
2. Corma A. From microporous to mesoporous molecular sieve materials and their use in catalysis. *Chemical Reviews.* 1997;97(6): 2373–2420.
3. Kerstens D, Smeyers B, Waeyenberg JV, Zhang Q, Yu J, Sels BF. State of the art and perspectives of hierarchical zeolites: practical overview of synthesis methods and use in catalysis. *Advanced Materials.* 2020;32(44): 2004690.
4. Koohsaryan E, Anbia M. Nanosized and hierarchical zeolites: A short review. *Chinese Journal of Catalysis.* 2016;37(4): 447–467.
5. Yue MB, Yang N, Jiao WQ, Wang YM, He MY. Dry-gel synthesis of shaped binderless zeolites composed of nanosized ZSM-5. *Solid State Sciences.* 2013; 20: 1–7.
6. Mitchell S, Michels NL, Pérez-Ramírez J. From powder to technical body: the undervalued science of catalyst scale up. *Chemical Society Reviews.* 2013;42(14): 6094–6112.
7. Liu B, Zhu X, Zhao J, Wang D, Ma W. A study into the γ-Al_2O_3 binder influence on nano-H-ZSM-5 via scaled-up laboratory methanol-to-hydrocarbon reaction. *Catalysts.* 2021;11(10): 1140.
8. Subero-Couroyer C, Ghadiri M, Brunard N, Kolenda F. Weibull analysis of quasi-static crushing strength of catalyst particles. *Chemical Engineering Research and Design.* 2003;81(8): 953–962.

9. Mik IA, Klenov OP, Kazakov MO, Nadeina KA, Klimov OV, Reshetnikov SI, Noskov AS. Guard of Catalysts for the Hydrotreating of Oil Fractions to Remove Solid Particles: Experimental Studies and Calculations. *Catalysis in Industry.* 2024;16(3): 330–338.
10. Yang K, Zhang D, Zou M, Yu L, Huang S. The known and overlooked sides of zeolite-extrudate catalysts. *ChemCatChem.* 2021;13(6): 1414–1423.
11. Zhao L, Zhao Y, Wang S, Yue H, Wang B, Lv J, Ma X. Hydrogenation of dimethyl oxalate using extruded Cu/SiO_2 catalysts: mechanical strength and catalytic performance. *Industrial & Engineering Chemistry Research.* 2012;51(43): 13935–13943.
12. Fakin T, Ristić A, Mavrodinova V, Logar NZ. Highly crystalline binder-free ZSM-5 granules preparation. *Microporous and Mesoporous Materials.* 2015;213: 108–117.
13. Shihabi DS, Garwood WE, Chu P, Miale JN, Lago RM, Chu CT, Chang CD. Aluminum insertion into high-silica zeolite frameworks: II. Binder activation of high-silica ZSM-5. *Journal of Catalysis.* 1985;93(2): 471–474.
14. Freiding J, Patcas FC, Kraushaar-Czarnetzki B. Extrusion of zeolites: Properties of catalysts with a novel aluminium phosphate sintermatrix. *Applied Catalysis A: General.* 2007;328(2): 210–218.
15. Lakiss L, Gilson JP, Valtchev V, Mintova S, Vicente A, Vimont A, Bedard R, Abdo S, Bricker J. Zeolites in a good shape: Catalyst forming by extrusion modifies their performances. *Microporous and Mesoporous Materials.* 2020;299: 110114.
16. Jacobs PA, Flanigen EM, Jansen JC, Bekkum HV. *Introduction to zeolite science and practice*. 2nd ed. Amsterdam: Elsevier; 2001.
17. Wu D, Tang M. Effects of process factors on extrusion of hierarchically porous ZSM-5 zeolite. *Powder Technology.* 2019;352: 79–90.
18. Gallei E, Schwab E. Development of technical catalysts. *Catalysis Today.* 1999;51(3-4): 535–546.
19. Richardson JT. *Principles of catalyst development.* New York: Springer; 2013.
20. Li Y, Li X, Chang L, Wu D, Fang Z, Shi Y. Understandings on the scattering property of the mechanical strength data of solid catalysts: A statistical analysis of iron-based high-temperature water-gas shift catalysts. *Catalysis Today.* 1999;51(1): 73–84.
21. Rebinder PA. *Surface phenomena in disperse systems; Physico-chemical mechanics: Selected works (in Russian)*. Moscow: Science; 1979. (In Russian)
22. Wu D, Zhou J, Li Y. Mechanical strength of solid catalysts: Recent developments and future prospects. *AIChE Journal.* 2007;53(10): 2618–2629.
23. Andrew SPS. Theory and practice of the formulation of heterogeneous catalysts. *Chemical Engineering Science.* 1981;36(9): 1431–1445.
24. Couroyer C, Ghadiri M, Laval P, Brunard N, Kolenda F. Methodology for investigating the mechanical strength of reforming catalyst beads. *Oil & Gas Science and Technology.* 2000;55(1): 67–85.
25. Krasnitckii SA, Sheinerman AG, Gutkin MYu. Brittle vs ductile fracture behavior in ceramic materials at elevated temperature. *Materials Physics and Mechanics.* 2024;52(2): 82–89.
26. Sheinerman AG. A model for the temperature dependence of the fracture strength of ceramic matrix composites. *Materials Physics and Mechanics.* 2025;53(5): 35–41.
27. Denny PJ, Twigg MV. Factors determining the life of industrial heterogeneous catalysts. *Studies in Surface Science and Catalysis.* 1980;6: 577–599.
28. Bemrose CR, Bridgwater J. A review of attrition and attrition test methods. *Powder Technology.* 1987;49(2): 97–126.
29. Li Y, Wu D, Zhang J, Chang L, Wu D, Fang Z, Shi Y. Measurement and statistics of single pellet mechanical strength of differently shaped catalysts. *Powder Technology.* 2000;113(1-2): 176–184.
30. Griffith AA. The phenomena of rupture and flow in solids. *Philosophical Transactions of the Royal Society of London.* 1921;221(582-593): 163–198.
31. Knudsen FP. Dependence of mechanical strength of brittle polycrystalline specimens on porosity and grain size. *Journal of the American Ceramic Society.* 1959;42(8): 376–387.
32. Ermolaeva YuV, Krasnitckii SA, Gutkin MYu. Temperature dependence of linear fracture mechanics parameters in ceramics: a finite element study. *Materials Physics and Mechanics.* 2025;53(6): 1–11.
33. Ignateva EV, Krasnitckii SA, Sheinerman AG, Gutkin MY. The finite element analysis of crack tolerance in composite ceramics. *Materials Physics and Mechanics.* 2023;51(2): 21–26.
34. Wu DF, Zhou JC, Li YD. Distribution of the mechanical strength of solid catalysts. *Chemical Engineering Research and Design.* 2006;84(12): 1152–1157.

35. Hutchings GJ. Crushing strength as a diagnostic test for catalysts. *Journal of Chemical Technology & Biotechnology.* 1986;36(6): 255–258.
36. American Society for Testing and Materials. ASTM D6175-03. *Standard test method for radial crush strength of extruded catalyst and catalyst carrier particles.* ASTM International; 2010.
37. American Society for Testing and Materials. ASTM D4179-11. *Standard Test Method for Single Pellet Crush Strength of Formed Catalysts and Catalyst Carriers*. ASTM International; 2011.
38. Bergman B. On the estimation of the Weibull modulus. *Journal of Materials Science Letters.* 1984;3(8): 689–692.
39. Wu D, Li Y. Effects of the impregnating and drying process factors on the mechanical properties of a PCoMo/Al_2O_3 hydrotreating catalyst. *Studies in Surface Science and Catalysis.* 2000;143: 101–109.
40. Madjoubi MA, Bousbaa C, Hamidouche M, Bouaouadja N. Weibull statistical analysis of the mechanical strength of a glass eroded by sand blasting. *Journal of the European Ceramic Society.* 1999;19(16): 2957–2962.
41. Trustrum K, Jayatilaka ADS. Applicability of Weibull analysis for brittle materials. *Journal of Materials Science.* 1983;18(9): 2765–2770.
42. Wilson DM. Statistical tensile strength of NextelTM 610 and NextelTM 720 fibres. *Journal of Materials Science.* 1997;32(10): 2535–2542.
43. Weibull W. A statistical distribution function of wide applicability. *Journal of Applied Mechanics.* 1951;3(8): 689–692.
44. Salem S, Salem A. A novel design for clean and economical manufacturing new nano-porous zeolite based adsorbent by alkali cement kiln dust for lead uptake from wastewater. *Journal of Cleaner Production.* 2017;143: 440–451.
45. Salem A, Sene RA. Optimization of zeolite-based adsorbent composition for fabricating reliable Raschig ring shaped by extrusion using Weibull statistical theory. *Microporous and Mesoporous Materials.* 2012;163: 65–75.
46. Guo M, Wang Y, Xie Z, Tan KB, Guo F, Sun K, Jiang J, Zhan G. Preparation and extrusion of ZSM-5 based on biomass templates for enhanced mechanical properties and catalytic pyrolysis performance. *Chinese Journal of Chemical Engineering.* 2025;80: 47–60.
47. Tian C., Wu D. Application of Response Surface Methodology for the Optimization of Drying Parameters of ZSM-5 Extruded Catalysts. *ChemistrySelect.* 2019;4(36): 10810–10818.
48. Tian C., Wu D. Mechanical properties of ZSM-5 extruded catalysts: calcination process optimization using response surface methodology. *Chemical Engineering Communications.* 2021;208(11): 1594–1606.
49. Lashchenko DI, Kukushkin RG, Danilova IG, Yakovlev IV, Bulavchenko OA, Lyulyukin AP, Rodina VO, Yakovlev VA. Effect of the alumina binder content on the mechanical strength and the Si/Al ratio in the zeolite framework in the shaped γ-Al2O3-ZSM-5 composites. *Materials Today Chemistry.* 2025;46: 102735.
50. Belopukhov E. A., Belyi A. S. Mechanical strength of composite supports for catalysts based on γ–Al_2O_3 and mordenite. *Procedia Engineering.* 2016;152: 735–741.
51. Shirazi L, Jamshidi E, Ghasemi MR. The effect of Si/Al ratio of ZSM-5 zeolite on its morphology, acidity and crystal size. *Crystal Research and Technology: Journal of Experimental and Industrial Crystallography.* 2008;43(12): 1300–1306.
52. Yu Z, Li S, Wang Q, Zheng A, Jun X, Chen L, Deng F. Brønsted/lewis acid synergy in H–ZSM-5 and H–MOR zeolites studied by 1H and 27Al DQ-MAS solid-state NMR spectroscopy. *The Journal of Physical Chemistry C.* 2011;115(45): 22320–22327.
53. GOST 34206-2017. *Plastics. Method for determining the shrinkage of thermosetting materials.* Moscow: Standards Publishing House; 2017. (In Russian)
54. Li Y, Wu D, Chang L, Shi Y, Wu D, Fang Z. A model for the bulk crushing strength of spherical catalysts. *Industrial & Engineering Chemistry Research.* 1999;38(5): 1911–1916.
55. Trustrum K, Jayatilaka ADS. On estimating the Weibull modulus for a brittle material. *Journal of Materials Science.* 1979;14(5): 1080–1084.
56. Wu D, Li Y, Zhang J, Chang L, Wu D, Fang Z, Shi Y. Effects of the number of testing specimens and the estimation methods on the Weibull parameters of solid catalysts. *Chemical Engineering Science.* 2001;56(24): 7035-7044.
57. Papargyris AD. Estimator type and population size for estimating the Weibull modulus in ceramics. *Journal of the European Ceramic Society.* 1998;18(5): 451–455.
58. Sullivan JD, Lauzon PH. Experimental probability estimators for Weibull plots. *Journal of Materials Science Letters.* 1986;5(12): 1245–1247.
59. American Society for Testing and Materials. ASTM D4464-15. *Standard Test Method for Particle Size Distribution of Catalytic Materials by Laser Light Scattering.* ASTM International; 2020.
60. Wu EL, Lawton SL, Olson DH, Rohrman AC, Kokotailo GT. ZSM-5-type materials. Factors affecting crystal symmetry. *Journal of Physical Chemistry.* 1979;83(21): 2777–2781.

61. Deng YQ, Yin SF, Au CT. Preparation of nanosized silicalite-1 and its application in vapor-phase Beckmann rearrangement of cyclohexanone oxime. *Industrial & Engineering Chemistry Research.* 2012;51(28): 9492–9499.
62. Alvarez AG, Viturro H, Bonetto RD. Structural changes on deactivation of ZSM-5. A study by X-ray powder diffraction. *Materials Chemistry and Physics.* 1992;32(2): 135–140.
63. Nikolopoulos N, Wickramasinghe A, Whiting GT, Weckhuysen BM. Alumina binder effects on the hydrothermal stability of shaped zeolite-based catalyst bodies. *Catalysis Science & Technology.* 2023;13(3): 862–873.
64. Soltani S, Zamaniyan A, Darian JT, Soltanali S. The effect of Si/Al ratio of ZSM-12 zeolite on its morphology, acidity and crystal size for the catalytic performance in the HTO process. *RSC Advances.* 2024;14(8): 5380–5389.
65. Sun M, Lin Z, Li W, Yue Y, Qian G, Zhang J. Influence of Si/Al ratio of ZSM-5 on Cu dispersion, its mechanism and efficiency in adsorbing CH3SH. *Materials Letters.* 2025;383: 138048.
66. Moghadam SA, Mazloom G, Akbari A, Banisharif F. Supported vanadium oxide catalyst over HY-zeolite-alumina composite fabricated by extrusion for oxidative desulfurization of dibenzothiophene. *Molecular Catalysis.* 2022;532: 112731.
67. Desmurs L, Cammarano C, Sachse A, Gimello O, Gaillard T, Barberat S, Blanquer S, Hulea V, Galarneau A. ZSM-5 monolithic microreactors with hierarchical porosity: Maximizing selective production of para-xylene. *Microporous and Mesoporous Materials.* 2024;377: 113201.
68. Jayatilaka ADS, Trustrum K. Statistical approach to brittle fracture. *Journal of Materials Science.* 1977;12(7): 1426–1430.
69. Wu D, Zhou J, Li Y. Unbiased estimation of Weibull parameters with the linear regression method. *Journal of the European Ceramic Society.* 2006;26(7): 1099–1105.
70. Klein CA. Characteristic strength, Weibull modulus, and failure probability of fused silica glass. *Optical Engineering.* 2009;48(11): 113401.
71. Khalili A, Kromp K. Statistical properties of Weibull estimators. *Journal of Materials Science.* 1991;26(24): 6741–6752.
72. Zwaag SVD. The concept of filament strength and the Weibull modulus. *Journal of Testing and Evaluation.* 1989;17(5): 292–298.
73. Zakeri M, Samimi A, Afarani MS, Salehirad A. Interaction between Weibull parameters and mechanical strength reliability of industrial-scale water gas shift catalysts. *Particuology.* 2017;32: 160–166.
74. Ismagilov ZR, Shkrabina RA, Koryabkina NA. *Alumina carriers: production, properties and application in catalytic processes of environmental protection*. Novosibirsk: BIC SB RUS; 1998. (In Russian)
75. Born ICVD. Mechanical strength of porous catalyst carriers. In: *Conference Organized by Koninklijke.* 1988. p.102–115.
76. Samimi A, Zakeri M, Maleki B, Mohebbi-Kalhori D. Experimental and statistical assessments of the mechanical strength reliability of gamma alumina catalyst supports. *Particuology.* 2015;21: 74-81.
77. Hargreaves JSJ, Munnoch AL. A survey of the influence of binders in zeolite catalysis. *Catalysis Science & Technology.* 2013;3(5): 1165–1171.
78. Whiting GT, Meirer F, Mertens MM, Bons AJ, Weiss BM, Stevens PA, Weckhuysen BM. Binder effects in SiO_2-and Al_2O_3-bound zeolite ZSM-5-based extrudates as studied by microspectroscopy. *ChemCatChem.* 2015;7(8): 1312–1321.
79. Soares VO, Daguano JK, Lombello CB, Bianchin OS, Gonçalves LM, Zanotto ED. New sintered wollastonite glass-ceramic for biomedical applications. *Ceramics International.* 2018;44(16): 20019–20027.
80. Li H, Elsayed H, Colombo P. Effect of particle size distribution and printing parameters on alumina ceramics prepared by Additive Manufacturing. *Ceramics International.* 2024;50(4): 6340–6348.
81. Chandan PB, Sankar MR. Tailoring the proportion of particle size to evaluate extrusion-based 3D printed alumina ceramics. *Materials Science and Engineering: B.* 2025;314: 117984.
82. Aranzabal A, Iturbe D, Romero-Sáez M, González-Marcos MP, González-Velasco JR, González-Marcos JA. Optimization of process parameters on the extrusion of honeycomb shaped monolith of H-ZSM-5 zeolite. *Chemical Engineering Journal.* 2010;162(1): 415–423.
83. Chu P, Liu H, Cai K, Liu Y, Li Y, Wang Y, Ma X. Influence of pseudoboehmite on the performance of shaped mordenite catalyst for dimethyl ether carbonylation. *Chemical Engineering Science.* 2023;272: 118607.